Jusami
Homepage: http://jusami.batan.go.id
Jurnal Sains Materi Indonesia
Akreditasi Nomor: 21/E/KPT/2018
Tanggal 9 Juli 2018
ISSN 1411-1098
E-ISSN 2614-087X

MICRO-CRYSTAL STRUCTURE OF AUSTENITIC STEEL $57Fe_{15}Cr_{25}Ni_{0.32}Mn_{0.96}Si$ AS TREATMENT RESULT AT 850 °C/5H-QUENCHING FOR HIGH TEMPERATURE MATERIAL APPLICATIONS

Parikin[1], Rudi[2], Sumaryo[1] and S. Ahda[1]
[1]*Center for Science and Technology of Advanced Material (PSTBM) - BATAN*
Kawasan Puspiptek, Serpong 15314, Tangerang Selatan
[2]*Department of Physics, FMIPA - University of Sumatera Utara*
Padang Bulan, Medan, Sumatera Utara 20155
E-mail: farihin@batan.go.id

Received: 1 August 2018 *Revised: 3 September 2018* *Accepted: 22 September 2018*

ABSTRACT

MICRO-CRYSTAL STRUCTURE OF AUSTENITIC STEEL $57Fe_{15}Cr_{25}Ni_{0.32}Mn_{0.96}Si$ AS TREATMENT RESULT AT 850 °C/5H - QUENCHING FOR HIGH TEMPERATURE MATERIAL APPLICATIONS. Austenite A2 type stainless steel series has been successfully synthesized using casting techniques at a temperature of over 1250 °C in induction furnaces that use electromagnetic inductive thermal systems. This steel is dedicated to component materials for multi-applications structures such as high temperature operating environments. Therefore, the material must be able to withstand mechanical loads, high temperatures, corrosion and irradiation. In order to increase the strength of the material, it is necessary to conduct temperature-quench treatment in several air, water and oil cooling media. Mineral elements extracted from Indonesian mine raw ore and commercial scrap materials, such as ferro scrap, ferro chrom, ferro nickel, ferro manganese, and ferro silicon, in granular form are melted into steel in the furnace. The titanium element is not added to this low carbon steel alloy. The OES-chemical composition of the alloy material in weight% is 57% Fe, 15% Cr, 25% Ni, 0.34% C and less than 0.1% impurity consisting of elements: titanium, phosphorus, copper, niobium and sulphur. The X-ray diffraction pattern shows that the as cast material has a fcc crystal structure with a lattice parameter of 3,632 Å. Meanwhile, two other samples; annealing and oil dipping, have lattice parameters similar to the normalization sample (air dye) of 3.580 Å. On the contrary, the lattice parameter of water dipping specimen is slightly lower than the as cast lattice parameter, which is 3.587 Å. The peak shifts of the planes (111) and (200) in the diffraction profile are very significant, around 0.63 degrees between the as cast specimens and the last two specimens. As cast microstructure reveals that austenite phase grains look large and represent an undamaged structure, with an average grain size of about 6 μm, while annealing specimens are even larger. The microstructure of normalized (air dyed) and oil specimens shows fine grains which are very different from those of water dipping specimens which show coarse grains. The viscosity η of cooling media has an important role in the formation of grain boundaries, because the level of temperature decrease is strongly influenced by the process of heat diffusion from high to low temperature space.

Keywords: Austenitic steel, $57Fe_{15}Cr_{25}Ni_{0.32}Mn_{0.96}Si$, X-Rays, Microstructure

ABSTRAK

STRUKTUR MIKRO-KRISTAL BAJA AUSTENITIK $57Fe_{15}Cr_{25}Ni_{0.32}Mn_{0.96}Si$ HASIL PELAKUAN TEMPERATUR 850 °C-5h - *QUENCHING* UNTUK APLIKASI MATERIAL TEMPERATUR TINGGI. Serial baja tahan karat austenit tipe A2 telah berhasil disintesis dengan menggunakan teknik pengecoran pada temperatur lebih dari 1250 °C dalam tungku induksi yang menggunakan sistem induktif termal elektromagnetik. Baja ini didedikasikan untuk bahan komponen struktur multi aplikasi seperti lingkungan operasi temperatur tinggi. Oleh karena itu, bahan harus mampu menahan beban mekanik, temperatur tinggi, korosi dan iradiasi. Agar kekuatan bahan dapat meningkat, perlu dilakukan treatment *temperatur-quench* dalam beberapa media pendingin udara, air dan oli. Unsur mineral yang diekstraksi dari bijih mentah tambang Indonesia

dan bahan scrap komersial, seperti: ferro scrap, ferro chrom, ferro nikel, ferro mangan, dan ferro silikon, dalam bentuk granular dipadu-lelehkan menjadi baja dalam tungku. Unsur titanium tidak ditambahkan kedalam paduan baja karbon rendah ini. Komposisi OES-kimia bahan paduan dalam % berat adalah 57% Fe, 15% Cr, 25% Ni, 0,34% C dan kurang dari 0,1% impuritas yang terdiri dari unsur-unsur: titanium, fosfor, tembaga, niobium dan sulfur. Pola difraksi sinar-X menunjukkan bahwa bahan *ascast* memiliki struktur kristal fcc dengan parameter kisi 3,632 Å. Sementara itu, dua sampel lain; anil dan celup minyak, memiliki parameter kisi mirip dengan sampel normalisasi (celup udara) sebesar 3,580 Å. Sebaliknya, parameter kisi spesimen celup air sedikit lebih rendah dari parameter kisi *ascast*, yaitu 3,587 Å. Pergeseran puncak bidang (111) dan (200) dalam profil difraksi, sangat signifikan, sekitar 0,63 derajat antara spesimen *ascast* dan dua spesimen terakhir. Struktur mikro *ascast* mengungkapkan bahwa butir fasa austenit terlihat besar dan menggambarkan struktur tak-rusak, dengan ukuran butir rata-rata sekitar 6 μm, sedangkan spesimen anil lebih besar lagi. Struktur mikro spesimen normalisasi (celup udara) dan minyak menunjukkan butir halus yang sangat berbeda dengan spesimen celup air yang menunjukkan butiran kasar. Sifat kekentalan (*viscosity, η*) media pendinginan memiliki peran penting dalam pembentukan batas butir, karena tingkat penurunan temperatur sangat dipengaruhi oleh proses difusi panas dari ruang bertemperatur tinggi ke rendah.

Kata kunci: Baja austenitik, $57Fe_{15}Cr_{25}Ni_{0.32}Mn_{0.96}Si$, Sinar-X, Strukturmikro

INTRODUCTION

The need for steel especially in the nuclear field is very much considered, particularly as a construction material for reactor structures operating in high temperature environments, both for the primary, secondary and tertiary zones. To meet high safety standards, the steel material needed must have a longterm resistance to: load, high pressure temperature, corrosion and irradiation. Literally, steel is a mixture of carbon with hard and strong coarse iron, and other elements are usually added for the purpose of engineering materials. In general, the definition of steel it-self is an alloy of iron (Fe) and carbon (C), where iron is the basic element and carbon is the main alloying element. Therefore, nowadays steel is widely used as a structural material for construction and manufacture [1].

The novelty in the study is a series of austenitic steels which had been made independently using the casting method, with a high Cr-Ni composition with low carbon content of about 0.34% by weight [2]. Two types of austenitic steel have been made, namely: steel A1 and A2 which are a mixture of local components. The aim of synthesizing steel is to create a new type of steel with higher chromium-nickel content and ductile properties and significantly increase corrosion resistance. Generally, stainless steel (SS) is made by adding a minimum of 10% chromium (Cr). SS then forms a chrome sesquioxide based surface. This oxide attaches to SS surface and can prevent further corrosion. This compound locks the material into the ferrite phase which functions as a body centered cubic (bcc) and is quite strong but not too resilient. Nickel (Ni) is often added to SS to change the structure into a more tenacious austenite phase and can increase high temperature oxidation resistance. One of the most common SS contains 18% Cr and 8% Ni [3] and is used for all needs from industrial piping to spoons and forks. This steel is known as SS 303 or SS 304 type. The type of austenitic stainless steel synthesized is A2 type [2] with chemical composition $57Fe_{15}Cr_{25}Ni_{0.32}Mn_{0.96}Si$ in% wt. Austenitic steels generally contain Cr 17-25% with other ingredients, ie with 8-20% Ni. In this austenite phase, steel has a face centered cubic (fcc) structure. The existence of the phase content greatly determines the characteristics of the material itself. Materials can be developed through high temperature treatment [4]. The crystallographic system of materials shows that the solubility of carbon in the austenite phase must be greater than the solubility in the ferrite phase (bcc). Geometric and solubility numbers can be calculated by comparing the amount of space in the austenite and ferrite phase intensities. In studies conducted on austenitic steel (A2 type) the mechanical properties have been observed such as: formability with cold rolling process, weldability and residual stress [5]. The average rigidity of this material is around 160 HVN (84 HRC). A recent study reported that A2 type steel showed very good corrosion rates, almost 0.088 mm per year [6].

This super austenitic alloy is a new type of austenitic steel, which contains several alloy elements, such as chrome, nickel, manganese, silicon and carbon. Ti element is added to show relatively better pitting corrosion [7,8], while the elements of phosphor, copper, niobium and sulphur are impurities contained in raw materials. This novelty of steel is designed to be able to be in a high temperature operating environment and also has high corrosion resistance, so that the Cr-Ni content is very extreme, unlike steel in the market (SS-304).

In this study, A2 steel material is one of the candidates to be applied to the secondary tertiary zones and can compete with other types of steel. Therefore it is necessary to explore and develop the application of this steel capability. The mechanical properties of materials can be engineered by providing heat treatment; among others, with the 'quench' technique. Quenching is the process of cooling metal quickly at a certain rate. The quenching process in this study was carried out

around the austenite temperature, that is: 850 °C [6]. This process was carried out to increase the value of rigidity, strength, toughness and formability of the material [9]. This effect can change the crystals and microstructure of materials. Changes can be observed well with diffraction techniques that are tailored by microscopic analysis using Optical Electron Microscopy (OM-EM).

The purpose of this study was to find out the characteristics of microstructure and austenitic steel crystals $57Fe_{15}Cr_{25}Ni_{0.32}M_{0.96}Si$ which were given rapid heating and cooling, in different viscosity media, i.e.: air, water and lubricating oil (oil; SAE 20-40), and compared with samples annealed and ascast as a reference.

EXPERIMENT METHOD

The research work chart is listed in Figure 1. Austenitic steel material of $57Fe_{15}Cr_{25}Ni_{0.32}Mn_{0.96}Si$ is the research object that has been created or synthesized by casting methods, as described in the literature [2]. The alloy material is melted in an induction furnace with a temperature of more than 1250 °C. The material chemical composition in wt% is shown in Table 1. Measurement of elemental composition was carried out using Swiss Optical Emission Spectrometry (OES) made in 1996 at Bandung Polytechnic and Manufacturing [2] with specially made samples, which had dimensions of 2.5 x 2.5 x 12 cm^3.

Austenitic steel material is cut into 5 parts using a diamond wafering cutter with dimensions of 1 x 1 x 0.2 cm^3. The quenching process is carried out by heating the sample from room temperature to a temperature of 850 °C. After reaching 850 °C, it is then held for 5 hours and each sample is dipped directly into the air, water and oil media. The surface of the sample is then smoothed consecutively using abrasive paper and paste until the surface is completely devoid of scratches left behind, smooth and shiny.

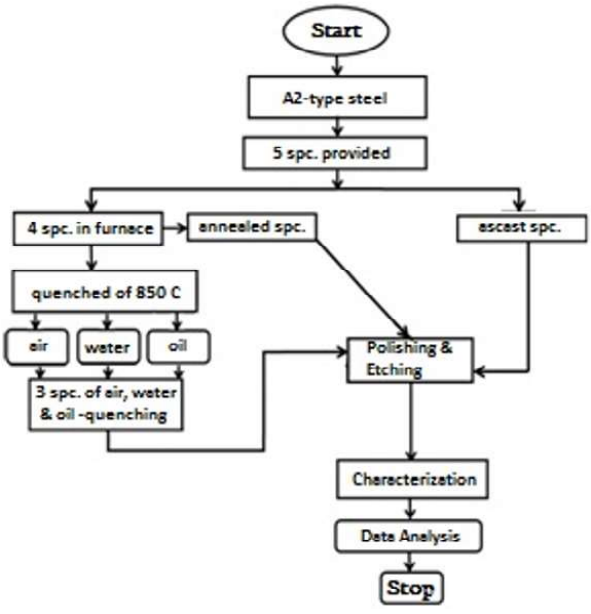

Figure 1. Research work chart/scheme.

Table 1. The chemical composition of austenitic steel in this study, resulted from optical emission spectroscopy (OES).

Elemental Composition (%wt.)										
Fe	Cr	Ni	Mn	Si	C	Ti	S	P	Cu	Nb
57.74	15.42	25.01	0.32	0.96	0.34	< 0.1				

Meanwhile, microstructure observation was conducted with standard procedures [10,11]. Characterization was carried out using Optical Microscope and Electron Microscope (SEM-JEOL type JSM-6510LA). SEM images were recorded by a secondary electron detector (SEI) on the acceleration energy of the main laser beam source in the form of tungsten wire with a maximum of 20 keV with a fixed working distance (WD) at 10 mm. WD value is setup to get the EDX spectrum in the best condition.

EDX is taken at an average dead time value of between 20% and 40%. More detailed information has been discussed in previous publications [10]. After going through the surface etching process the test sample becomes a dop, using an optical microscope, the surface microstructure can be observed. Furthermore, the crystal structure was verified by collecting reflection intensity using an X-ray diffractometer. Cu target wavelength is used in measurements with PANalytical's Empyrean X-ray Diffractometer located in PSTBM-BATAN. The samples are scanned in a range of 2θ from 40 to 100 degrees with a counting step of 0.02 degrees and preset count mode = 2.

Semi quantitatively (EDX), the composition of steel samples was also observed using JSM-6510LA SEM-JEOL in PSTBM BATAN. The microstructure image capturing process is carried out using a secondary electron (SE) detector on the maximal primary electron beam acceleration energy from a tungsten wire source of 20 keV with a working distance (WD) kept constant as far as 10 mm.

RESULTS AND DISCUSSION

Crystal Structure

Figure 2 shows an X-ray diffractogram for A2 type steel taken using PANalytical XRD with Cu target (λ = 1.54 Å) in the range of 2θ from 40° to 100° . Five characteristic peaks appeared in 5 diffraction patterns of the samples produced, including 3 samples with different quenching treatments. Fields of reflection (111), (200), (220), (311) and (222) are clearly visible and scattered at diffraction angles (2θ) consecutively: 43,5° ; 51° ; 75° ; 91° and 96,5° . The Miller index [13] is grouped on all even or all odd numbers for all sample treatments where the face center cubic (fcc) crystal is a representative space group.

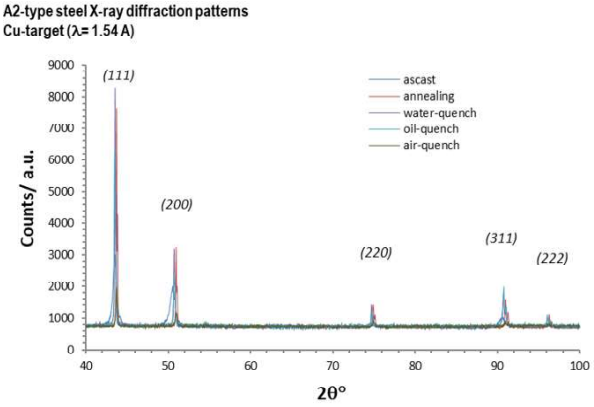

Figure 2. Diffraction pattern of A2 type steel with and without temperature treatment of 850 °C for 5 hours.

The peak pattern of ascast sample is wider than the others (see fields (111) and (200) in Figure 3). Samples annealed for 30 minutes and samples quenched in air, water and oil media showed very sharp peaks, even the second wavelength ($K\alpha_2$) appeared at each primary peak ($K\alpha_1$). In addition to the absence of a filter for $K\alpha_2$ in an X-ray diffraction system, in this case, if the surface area and time of X-ray irradiation in the material are the same, the integrated intensity (area below the line) of the low widened peak and high sharp peak is the same. The crystallite size of the low widened peak is smaller than the high sharp peak. The annealing process can increase the size of the material crystal/granule. As the crystal size is relatively large, the peak is sharp and high.

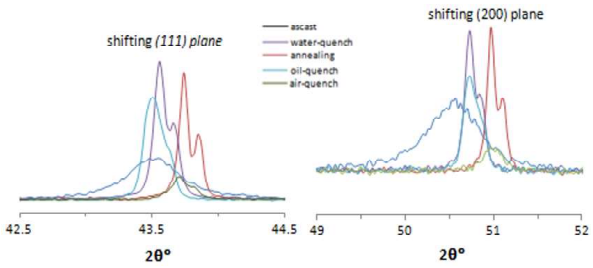

Figure 3. Diffraction pattern series of steel type A2 for (111) and (200).

Quenching treatment in various media may affect the dynamics of crystal lattice. The phenomenon of stretching and shrinkage of the length of the crystal lattice is very likely to occur. As detected in 5 steel samples in this study, the crystal lattice was seen stretching and shifting around the diffraction angle 2θ. The top position can move to the left and right. It can be seen in Figure 3 that, if the ascast profile is assumed to be the origin sample, then if sorted from annealed sample, air- (normalized), water- and oil- quench, the peak profile looks to move to the right then returns to the left in the initial position (ascast). Table 2 lists the profile smoothing parameters, which inform/support the shifting phenomenon. The X-ray diffraction pattern shows that ascast material has a fcc crystal structure with a

Table 2. Profile smoothing parameters on reflection field (111).

Spesimen	*A (Å)*	2θ (°)	Δ2θ (°)	*Fwhm* (°)	R_{wp} (%)	S
ascast*	3,632	43.099	-	0.3887	4.36	1.35
anil	3.582	43.732	0.633	0.0819	5.39	1.49
q-udara	3.580	43.750	0.284	0.1141	4.17	1.07
q-air	3.587	43.662	0.563	0.0801	4.70	1.42
q-oli	3.581	43.738	0.639	0.1246	4.69	1.42

**ref.*, *q=quench*

lattice parameter of 3,632 Å. Meanwhile, two samples annealed and quenched in oil, are very identical to the quench air lattice parameter (normalization) around 3.580 Å. The sample quenched in water has a lattice parameter slightly longer than the ascast lattice parameter, which is 3.587 Å.

The peak shifts (111) and (200) in profile diffraction are shown to be very significant, about 0.63 degrees between the ascast sample and the last two samples; annealed and quench in lubricating oil. These shifts can have an impact on changes in lattice parameters and can affect the stretch of the crystal lattice, and cause the emergence of residual stress in the material [5]. Figure 3 shows the phenomenon of peak shift in 2θ from the annealed sample sequence, air- (normalization), water- and oil- quench. The air-quench sample may have the highest residual stress due to the farthest shift value (1,284°) according to the formulation [12] $\Delta 2\theta = -2\,\varepsilon \tan\theta$ [12], where ε is the lattice stretch component proportional to the calculated residual stress σ. This sample is likely to be easily attacked by environmental corrosion faster than other samples (experiencing earlier fragility). This high temperature corrosion rate in steel materials has been discussed in the literature [6].

Microstructure

Figure 4 shows the optical microstructure of steel (a) as-cast and (b) annealed sample with 100x magnification. As-cast samples have round granules of 6 μm [12]. Black spots are also seen distributed on the material surface. Diagonal line strokes still appear in micrographs. In Figure 4(b), the grain swells after the sample is annealed at a temperature of 850 °C. Matrix grains undergo rearrangement where small grains join together to form large colonies. The grain orientation seems to still lead to fields (111) and (200). The diffraction

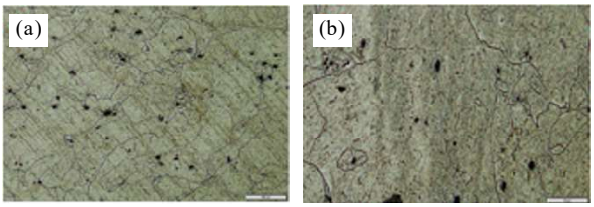

Figure 4. Microstructure (OM) of samples (a). ascast and (b). annealed at 850 °C-5 hours with 100x magnification.

pattern of the annealed sample shows a very high intensity on reflection (111) and (200).

Figure 5 shows the material microstructure after treatment at 850 °C for 5 hours from (a) air-quench (normalization), (b) samples of water-quench and (c) samples of oil-quench with Optical Microscopes (OM-100x). Corrosion of demin water as long as grain boundaries is clearly observed on the steel surface. Coarse lines are seen on the sample surface of the air- and water-quench, but on the surface of the oil-quench, the grain boundaries appear very fine, due to differences in quench media viscosity (ηa < ηw < ηo) [14]. From these conditions, temperature decrease in oil media consecutively falls down faster than in water and air media. The same thing in water media when compared to air media. So, the granule formation process in oil media looks finer than in water and air media. The homogeneity of fluids can also cause different effects. When cooled (quenched) in air, it is as if demin water can attack certain parts of the sample surface. While being dipped in water, demin water helps erode grain boundaries (such as irrigation basins), while being immersed into lubricating oil, demin water uniformly attacks the entire surface of the sample and quickly covers the surface. Meanwhile, the ascast sample and the annealed sample showed no significant changes that occurred in the surface images. Observation of microstructure with an optical microscope does not indicate information on damage and changes in grain size on the material surface due to the cooling process. Phase analysis (see Figure 2) with X-ray diffraction also does not show the presence of the corrosion product phase identified [8].

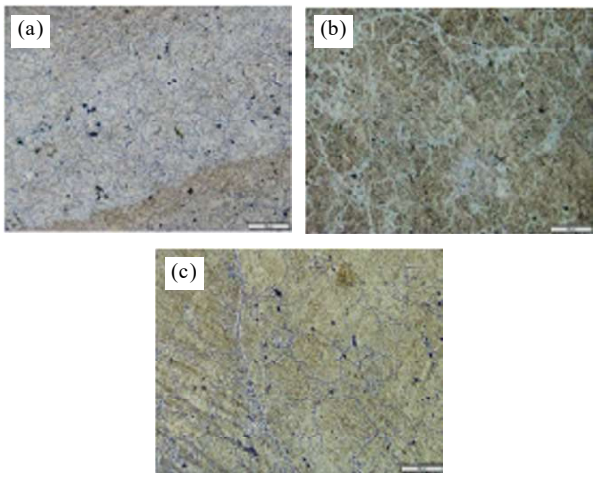

Figure 5. Microstructure (OM) of (a). air-quench (normalization), (b). samples of water-quench and (c). oil-quench with 100x magnification, obtained temperature treatment of 850 °C for 5 hours.

The EDX spectrum [15] as shown in Figure 6 shows that the carbon element (C) does not occupy the steel matrix. The carbon element is concentrated at the grain boundary, forming a chrome carbide precipitate at the grain boundary where the location has the lowest energy. Meanwhile, Si elements (1.24% by weight) and Ni (13.66% by weight) were detected to prefer to occupy the surface (grains) of this steel matrix, compared to grain boundary. This can be seen from the quantity comparison of Si (0.81% by weight) and Ni (11.38% by weight) in grain boundary to be less than in grains, i.e.:

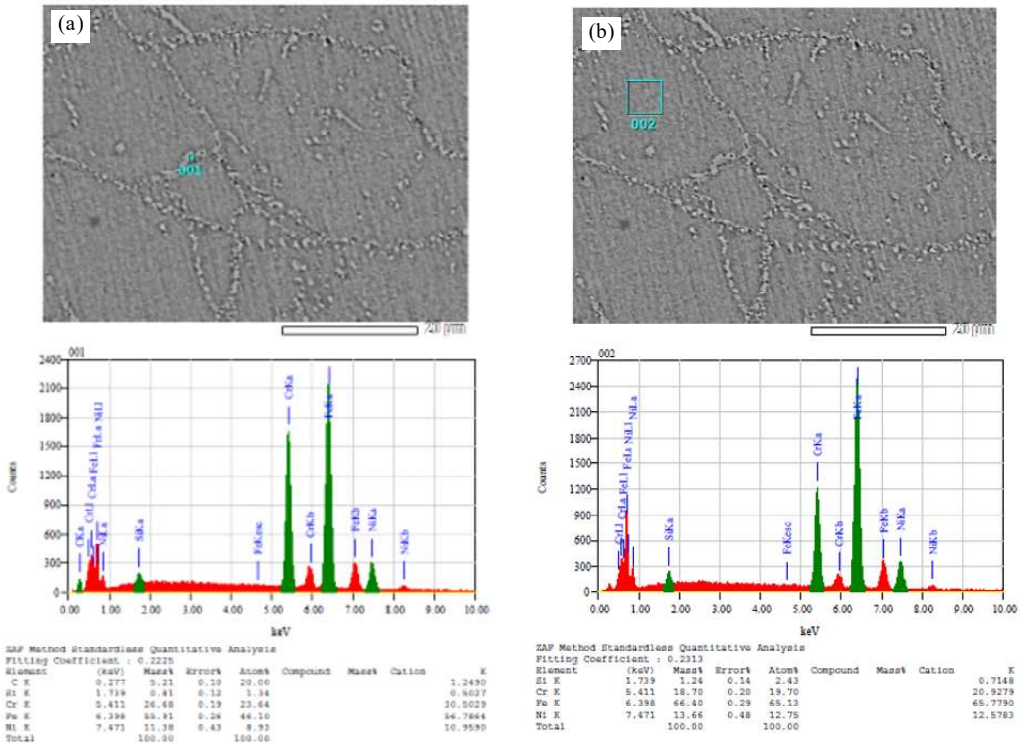

Figure 6. SEM-EDX spectrum on (a). grain boundaries and (b). ascast sample matrix.

Si element (1.24% by weight) and Ni (13.66% by weight). Some coagulations (precipitates) look like forming colonies in long and circular sequences, surrounding a steel matrix. Carbon seems to prefer reacting with the Cr element to form a chrome carbide compound (Cr_xC_y). Another study reported [15,16] that the effect of $Cr_{23}C_6$ compound can reduce material toughness as it initiates cracks.

Whereas for steel samples quenched similarly with ascast steel, it only differs at finer grain boundaries. It is assumed that the heating process to a temperature of 850 °C and is held for 30 minutes, then cooled quickly in air, water and oil media, is capable of effecting the formation of narrower grain boundaries.

CONCLUSION

The X-ray diffraction pattern shows that austenitic steel which has fcc crystal structure does not change due to quenching process, only the lattice parameter changes. As-cast has a lattice parameter of about 3.632 Å. Meanwhile for two samples, i.e.: annealing and quench of lubricating oil (oil) is very similar to the air quench (normalization) lattice parameter of around 3.580 Å. While the water quench sample has a lattice parameter that is slightly shorter than the ascast lattice parameter, which is 3,587Å. Peak shifts from fields (111) and (200) in diffraction profiles were very significant, approximately 0.63 degrees between the ascast samples and the last two samples: annealed and oil-quench.

The microstructure of ascast steel shows austenite phase grain that looks large with an average grain size of about 6 μm, while the annealed sample is even greater. The micro-structure of the air- and oil-quench samples showed fine austenite phase granules which were very different from the water quench microstructure which showed austenitic phase with coarse grain.

Viscosity (η) of cooling media has an important role in the formation of grain boundaries, because the rate of decrease in temperature is strongly influenced by the diffusion of heat from low temperature space to a high temperature space in the material.

ACKNOWLEDGEMENT

The author thanks the head of PSTBM and BSBM, and: Drs. Bambang Sugeng, M.T., Imam Wahyono, S.ST. and Agus Sujatno A.Md. for their kindness and assistance. In addition, the author would like to thank you for the financial support from DIPA 2016.

REFERENCES

[1]. M.J. Schneider, M.S. Chatterjee and B.S. Lampman. "Introduction to Surface Hardening of Steels, Heat Treating", J. Dossett and G.E. Totten, editors, ASM Handbook, Volume 4A, New York: McGraw-Hill, pp. 389-398, 2013.

[2]. N. Effendi, A. K. Jahja, Bandriana and W. A. Adi. "Some Data of Second Sequence Non Standard Austentic Ingot A2-Type", Urania, Scientific Journal of Nuclear Fuel Cycle vol. 18-1, pp. 48-58, 2012.

[3]. M. Weiser. "Stainless Steel vs. Carbon Steel Tools", Available: http://www.inlandbonsai.com/ articles/ steel/steel.pdf, [Aug. 1, 2017].

[4]. J. Gorka. "Microstructure and properties of the high-temperature (HAZ) of thermo-mechanically treated S700MC high-yield-strength steel", Materials Tehnology, vol. 50, pp. 617-621, 2016.

[5]. Parikin, A.H. Ismoyo, R. Iskandar and A. Dimyati. "Residual Stress Measurements on The TIG-Weldjoint of 57Fe15Cr25Ni Austenitic Steel for Structure Material Applications by Means X-Ray Diffraction Techniques", Makara Journal of Technology, University of Indonesia, vol. 21-2, pp. 49-57, 2017.

[6]. Parikin, B. Sugeng, M. Dani dan S. G. Sukaryo. "Ketahanan Oksidasi Baja Super Austenitik 15%Cr-25%Ni pada Temperatur 850 °C", Jurnal Sains Materi Indonesia (Indonesian Science and Materials Journals), vol. 18-4, pp. 179-184, 2017.

[7]. A. Grajcar, A. Plachcinska, S. Topolska and M. Kciuk. "Effect of thermomechanical treatment on the corrosion behavior of Si and Al-containing high-Mn austenitic steel with Nb and Ti microaddition", Materials Tehnology, vol. 49, pp. 889–894, 2015.

[8]. R. T. Loto. "Pitting corrosion evaluation and inhibition of stainless steels: A review", Journal of Materials and. Environmental Science, vol. 6-10, pp. 2750-2762, 2015.

[9]. S. Imano, J. Sato, H. Kamoshida, T. Shibayama, and A. Ota. "Alloy Design and Innovative Manufacturing Technology of High-Strength Ni-base Wrought Alloy for Efficiency Improvement in Thermal Power Plants". Mitsubishi Heavy Industry Technology Reviews, vol. 52-2, pp.32-38, 2015.

[10]. M. Dani, Parikin, A.K. Jahja, A. Dimyati, R. Iskandar and J. Mayer. "Investigation on Precipitations and Defects of the Fe-24Cr-2Si-0.8Mn Ferritic Super Alloy Steel, Jurnal Sains Materi Indonesia (Indonesian Science and Materials Journals), vol. 18-4, pp. 173-178, 2017.

[11]. T.L. Burnett, R. Kelley, B. Winiarski, L. Contreras, M. Daly A. Gholinia M.G. Burke and P.J. Withers. "Large Volume Serial Section Tomography by Xe Plasma FIB Dual Beam Microscopy", Ultramicroscopy, vol. 161, pp. 119–129, 2016.

[12]. Parikin, T.H. Priyanto, A.H. Ismoyo dan M.Dani. "Efek Rol Panas Pada Sifat Mekanik Plat Baja

15%Cr-25%Ni Bahan Struktur Reaktor (Hot Rolling Effects on Mechanical Properties of 15%Cr-25%Ni Steel Plate for Reactor Structure Materials)", Jurnal Sains Materi Indonesia (Indonesian Science and Materials Journals), vol. 16-1, pp. 22-28, 2015.

[13]. T.N. Blanton, J.A. Kaduk and Q. Johnson. "X-ray diffraction characterization of a distorted Debye–Scherrer film strip – the effect of deacetylation on cellulose triacetate and an improved structural model for cellulose II", Powder Diffraction, vol. 29-2, pp.108-112, 2014.

[14]. M. Dauda, L. S. Kuburi, D. O. Obada and R. I. Mustapha. "Effect of various quenching media on mechanical properties of annealed 0.509Wt%C-0.178Wt%Mn Steel", Nigerian Journal of Technology (NIJOTECH), vol. 34-3, pp. 506 – 512, 2015.

[15]. Parikin, M. Dani, A.K. Jahja, R. Iskandar, and J. Mayer. "Crystal Structure Investigation of Ferritic 73Fe24Cr2Si0.8Mn0.1Ni Steel for Multi-purpose Structural Material Applications". International Journal of Technology, vol. 9-1, pp. 78-88, 2018.

[16]. M. Dani, Parikin, A. Dimyati, A. K. Rivai, and R. Iskandar. "A New Precipitation-Hardened Austenitic Stainless Steel Investigated by Electron Microscopy" International Journal of Technology, vol. 9-1, pp. 89-98, 2018.